

KEK preprint 96-33

KEK TH-476

FERMILAB-PUB-96/130-T

## Direct $CP$ violations of $B$ meson via $\rho - \omega$ interference \*

Ryoji Enomoto<sup>a†</sup> and Masaharu Tanabashi<sup>a,b‡</sup>

<sup>a</sup>*National Laboratory for High Energy Physics, 1-1 Oho, Tsukuba, Ibaraki 305, Japan*

<sup>b</sup>*Fermilab, MS 106, P.O.Box 500, Batavia, IL 60510<sup>§</sup>*

(July 3, 2018)

### Abstract

We investigate  $B^{\pm,0} \rightarrow \rho^0(\omega)h^{\pm,0}$ , where  $\rho^0(\omega)$  decays to  $\pi^+\pi^-$  and  $h$  is any hadronic final states, such as  $\pi$  or  $K$ . We find large direct  $CP$  asymmetries via  $\rho - \omega$  interference. A possible determination of the weak phases, such as  $\phi_2 = \arg((V_{ud}V_{ub}^*)/(V_{td}V_{tb}^*))$  and  $\phi_3 = \arg((V_{us}V_{ub}^*)/(V_{ts}V_{tb}^*))$ , is also discussed. We show the feasibility to detect the  $CP$  asymmetries in these channels by assuming an asymmetric  $e^+e^-$  collider experiment.  $10^9$   $B\bar{B}$  events are required for the detection of this effect.

Typeset using REVTeX

---

\*submitted for publication.

†e-mail: enomoto@kekvox.kek.jp.

‡e-mail: tanabash@theory.kek.jp

§Address till August 25, 1996.

Although  $CP$  violation has been observed in the  $K^0-\bar{K}^0$  system since 1964, we have no evidence up to now of  $CP$  violation other than in the kaon system. For understanding the origin of the  $CP$  violation, however, we definitely need information concerning  $CP$  violations other than that in the  $K^0-\bar{K}^0$  system.

The standard model of the  $CP$  violation [1] predicts large  $CP$  asymmetries in the  $B$  meson system [2]. Many experimental attempts to detect  $CP$  violations of the  $B$  meson will be carried out towards the next century [3–5]. Thanks to the large number of its decay modes, a precise measurements of the  $B$ -meson  $CP$  asymmetries will supply much information for a deeper understanding of the origin of the  $CP$  violation, which will provide clues for the new physics beyond the standard model. For such a purpose, we need to consider the various  $B$ -meson  $CP$  asymmetries (as many as possible).

Unlike the  $CP$  violations in the neutral  $B$  meson, the  $CP$  asymmetry of the charged  $B$  meson can be caused solely by direct  $CP$  violations, which only occur through interference between two amplitudes having different weak and strong phases. In the standard model a weak-phase difference is provided by the different complex phase of the Kobayashi-Maskawa (KM) matrix elements [1] of the tree and penguin diagrams, while the strong phase is given by the absorptive parts of the corresponding diagrams.

To obtain a large direct  $CP$  asymmetry, which can be observed in future  $B$  factories, we need to consider a decay mode with a sufficiently large strong phase difference. We also need to know precisely the size of the strong-phase difference in order to extract the size of the weak phase difference (KM phase) from the observed direct  $CP$  asymmetry.

However, it is difficult to control such a large absorptive part (strong phase) in a perturbative manner. Nonperturbative resonance states, in which we know the behavior of the absorptive part by using the Breit-Wigner shape, are ideal places for this game. The  $CP$  violations via the radiative decays of  $B$  meson were predicted by Atwood and Soni [6,7]. The role of charmonium resonances in the  $CP$  violation of  $B^\pm$  decay was discussed by Eilam, Gronau and Mendel [8]. Lipkin discussed the use of  $\rho$ - $\omega$  interference as a trigger of the direct  $CP$  violation in neutral  $B$ -meson decay using a simple quark model analysis [9].

In this Letter we present a systematic analysis of the  $CP$  asymmetries in  $B^{\pm,0} \rightarrow \rho^0(\omega)h^{\pm,0} \rightarrow \pi^+\pi^-h^{\pm,0}$  via  $\rho\omega$  interference [10], where  $h$  is any hadronic final state, such as  $\pi$ ,  $\rho$ ,  $K$ ,  $K^*$ . We find large  $CP$  asymmetries at the interference region. We also show the feasibility of this method assuming a realistic luminosity and detector. Although the size of  $\rho\omega$  mixing is quite small, since it is triggered by the small isospin violation, an enhancement at the  $\omega$  pole can overcome this smallness at the  $\omega$  pole region. In addition, these decay modes are considered to have a reasonably large branching fraction, such as  $10^{-5}$  [11,12].

Figures 1 (a) and (b) are examples of quark level diagrams of the tree (a) and penguin (b) amplitudes for  $B^\pm \rightarrow \rho^0(\omega)\rho^\pm$ . Considering the quark components: while diagram (a) gives a final state of  $\rho^0 + \omega$ , diagram (b) contributes solely to a  $\omega$  meson. The standard model predicts a weak phase difference,  $\phi_2 = \arg((V_{ud}V_{ub}^*)/(V_{td}V_{tb}^*))$ . The absorptive part (strong phase) is provided by both the  $\rho\omega$  interference and the Bander-Silverman-Soni mechanism (the quark loop absorptive part in the penguin diagram) [13].

We start with a general strategy for evaluating the  $CP$  asymmetry in this system. The  $CP$  asymmetry is given by

$$a \equiv \frac{|A|^2 - |\bar{A}|^2}{|A|^2 + |\bar{A}|^2} = \frac{r(\cos(\delta + \phi) - \cos(\delta - \phi))}{1 + r^2 + r(\cos(\delta + \phi) + \cos(\delta - \phi))}, \quad (1)$$

where  $\delta$  and  $\phi$  are the strong and weak phases, respectively. The amplitudes ( $A$  and  $\bar{A}$ ) are

$$\begin{aligned} A &\equiv \langle \pi^+\pi^-h|\mathcal{H}^T|B\rangle + \langle \pi^+\pi^-h|\mathcal{H}^P|B\rangle = \langle \pi^+\pi^-h|\mathcal{H}^T|B\rangle [1 + re^{i\delta}e^{i\phi}], \\ \bar{A} &\equiv \langle \pi^+\pi^-\bar{h}|\mathcal{H}^T|\bar{B}\rangle + \langle \pi^+\pi^-\bar{h}|\mathcal{H}^P|\bar{B}\rangle = \langle \pi^+\pi^-\bar{h}|\mathcal{H}^T|\bar{B}\rangle [1 + re^{i\delta}e^{-i\phi}], \end{aligned}$$

with  $\mathcal{H}^T$  and  $\mathcal{H}^P$  being the tree and penguin Hamiltonians, respectively. The parameter  $r$  stands for the absolute value of penguin/tree ratio,

$$r \equiv \left| \frac{\langle \pi^+\pi^-h|\mathcal{H}^P|B\rangle}{\langle \pi^+\pi^-h|\mathcal{H}^T|B\rangle} \right|. \quad (2)$$

We assume that the vector meson contributions dominate over the continuum  $\pi^+\pi^-$  final state when the  $\pi^+\pi^-$  invariant mass is sufficiently close to the  $\omega$  meson mass  $m_\omega$ ,

$$\langle \pi^+\pi^-h|\mathcal{H}^{T,P}|B\rangle \simeq \langle \pi^+\pi^-|J_0^\mu|0\rangle \frac{\epsilon_\mu(\omega)}{g_\omega} \langle \omega h|\mathcal{H}^{T,P}|B\rangle + \langle \pi^+\pi^-|J_3^\mu|0\rangle \frac{\epsilon_\mu(\rho)}{g_\rho} \langle \rho h|\mathcal{H}^{T,P}|B\rangle, \quad (3)$$

where  $\epsilon_\mu(\omega/\rho)$  and  $g_{\omega/\rho}$  are the polarization vector and the decay constant of  $\omega/\rho$ , respectively. This assumption can be confirmed experimentally. For later convenience, we define  $\alpha$ ,  $\delta_\alpha$ ,  $\beta$ ,  $\delta_\beta$ ,  $r'$  and  $\delta_q$  as:

$$\alpha e^{i\delta_\alpha} \equiv \frac{\langle \omega h | \mathcal{H}^T | B \rangle}{\langle \rho h | \mathcal{H}^T | B \rangle}, \quad \beta e^{i\delta_\beta} \equiv \frac{\langle \rho h | \mathcal{H}^P | B \rangle}{\langle \omega h | \mathcal{H}^P | B \rangle}, \quad r' e^{i(\delta_q + \phi)} \equiv \frac{\langle \omega h | \mathcal{H}^P | B \rangle}{\langle \rho h | \mathcal{H}^T | B \rangle}, \quad (4)$$

with  $\delta_\alpha$ ,  $\delta_\beta$  and  $\delta_q$  being the strong phases (absorptive part) at short distance. These strong phases can be roughly evaluated from the quark loop diagrams [13]. By using these parameters, we obtain

$$r e^{i\delta} = r' e^{i\delta_q} \frac{\beta e^{i\delta_\beta} \langle \pi^+ \pi^- | J_3^\mu | 0 \rangle \frac{\epsilon_\mu}{g_\rho} + \langle \pi^+ \pi^- | J_0^\mu | 0 \rangle \frac{\epsilon_\mu}{g_\omega}}{\langle \pi^+ \pi^- | J_3^\mu | 0 \rangle \frac{\epsilon_\mu}{g_\rho} + \alpha e^{i\delta_\alpha} \langle \pi^+ \pi^- | J_0^\mu | 0 \rangle \frac{\epsilon_\mu}{g_\omega}}. \quad (5)$$

We now evaluate the long-distance hadronic  $\pi^+ \pi^-$  final state interaction at the  $\omega$  meson mass region using a simple model of  $\rho$ - $\omega$  mixing [14]:

$$\begin{aligned} \langle \pi^+ \pi^- | J_0^\mu | 0 \rangle &\sim g_{\rho\pi\pi} \frac{1}{m_\rho^2 - i\Gamma_\rho m_\rho - s} \left[ \frac{g_\omega}{3} \frac{e^2}{-s} g_\rho + g_{\rho\omega} \right] \frac{1}{m_\omega^2 - i\Gamma_\omega m_\omega - s} g_\omega, \\ \langle \pi^+ \pi^- | J_3^\mu | 0 \rangle &\sim g_{\rho\pi\pi} \frac{1}{m_\rho^2 - i\Gamma_\rho m_\rho - s} g_\rho, \end{aligned}$$

where  $|\omega\rangle$  and  $|\rho\rangle$  are defined as the isospin eigenstates and  $g_\omega$ ,  $g_\rho$ ,  $g_{\rho\omega}$  and  $g_{\rho\pi\pi}$  are the decay constants of the  $\omega$  and  $\rho$  mesons,  $\rho$ - $\omega$  mixing amplitude and  $\rho\pi\pi$  coupling, respectively. We thus obtain

$$\frac{\langle \pi^+ \pi^- | J_0^\mu | 0 \rangle \epsilon_\mu}{\langle \pi^+ \pi^- | J_3^\mu | 0 \rangle \epsilon_\mu} \simeq \frac{g_\omega}{g_\rho} \frac{g_\rho^2}{m_\omega^2 - i\Gamma_\omega m_\omega - s} \left[ \frac{g_\omega}{3} \frac{e^2}{-s} g_\rho + g_{\rho\omega} \right], \quad (6)$$

where  $s$  denotes the invariant mass square of  $\pi^+ \pi^-$ . The size of the mass mixing ( $g_{\rho\omega}$ ) can be evaluated from

$$\frac{\Gamma(\omega \rightarrow \pi^+ \pi^-)}{\Gamma(\rho \rightarrow \pi^+ \pi^-)} = \frac{1}{(m_\rho^2 - m_\omega^2)^2 + \Gamma_\rho^2 m_\rho^2} \left[ \frac{g_\omega}{3} \frac{e^2}{-m_\omega^2} g_\rho + g_{\rho\omega} \right]^2. \quad (7)$$

Putting the experimental values,  $\Gamma(\omega \rightarrow \pi^+ \pi^-) = 0.19\text{MeV}$ ,  $\Gamma(\rho \rightarrow \pi^+ \pi^-) = \Gamma_\rho = 150\text{MeV}$ , and  $\Gamma_\omega = 8.4\text{MeV}$  into Eq.(7), we find

$$\frac{g_\omega}{3} \frac{e^2}{-m_\omega^2} g_\rho + g_{\rho\omega} \simeq 0.63 \Gamma_\omega m_\omega, \quad (8)$$

where the sign is determined from  $e^+e^- \rightarrow \pi^+\pi^-$  near  $\rho$ -meson mass.

Plugging Eqs.(6) and (8) into Eq.(5), we can evaluate the behavior of the strong phase at the  $\omega$  meson mass region,

$$re^{i\delta} \simeq r'e^{i\delta_q} \frac{\beta e^{i\delta_\beta}(m_\omega^2 - i\Gamma_\omega m_\omega - s) + 0.63\Gamma_\omega m_\omega}{m_\omega^2 - i\Gamma_\omega m_\omega - s + 0.63\alpha e^{i\delta_\alpha}\Gamma_\omega m_\omega}. \quad (9)$$

In the ideal case, where  $(\alpha, \beta, \delta_q) = (0, 0, 0)$ , we thus obtain the maximum strong-phase difference at  $s = m_\omega$ .

We next roughly evaluate the sizes of these parameters  $(\alpha, \beta, r')$  of several decay modes. The effective weak Hamiltonian is given by:

$$\mathcal{H}^T = \frac{4G_F}{\sqrt{2}} V_{ub} V_{uq}^* \sum_{i=1}^2 c_i(\mu) O_i^{(u)}, \quad \mathcal{H}^P = -\frac{4G_F}{\sqrt{2}} V_{tb} V_{tq}^* \sum_{i=3}^6 c_i(\mu) O_i, \quad (10)$$

with

$$\begin{aligned} O_1^{(u)} &= \bar{q}_{L\alpha} \gamma^\mu u_{L\beta} \bar{u}_{L\beta} \gamma_\mu b_{L\alpha}, & O_2^{(u)} &= \bar{q}_{L\alpha} \gamma^\mu u_{L\alpha} \bar{u}_{L\beta} \gamma_\mu b_{L\beta}, \\ O_3 &= \bar{q}_{L\alpha} \gamma^\mu b_{L\alpha} \sum \bar{q}'_{L\beta} \gamma_\mu q'_{L\beta}, & O_4 &= \bar{q}_{L\alpha} \gamma^\mu b_{L\beta} \sum \bar{q}'_{L\beta} \gamma_\mu q'_{L\alpha}, \\ O_5 &= \bar{q}_{L\alpha} \gamma^\mu b_{L\alpha} \sum \bar{q}'_{R\beta} \gamma_\mu q'_{R\beta}, & O_6 &= \bar{q}_{L\alpha} \gamma^\mu b_{L\beta} \sum \bar{q}'_{R\beta} \gamma_\mu q'_{R\alpha}, \end{aligned} \quad (11)$$

with  $\alpha$  and  $\beta$  being color indices. The Wilson coefficients of these operators at the  $B$  meson mass scale ( $\mu = m_b = 5\text{GeV}$ ) are calculated as [15,16]:

$$\begin{aligned} c_1(\mu) &= -0.3125, & c_2(\mu) &= 1.1502, \\ c_3(\mu) &= 0.0174, & c_4(\mu) &= -0.0373, \\ c_5(\mu) &= 0.0104, & c_6(\mu) &= -0.0459. \end{aligned} \quad (12)$$

These coefficients receive finite renormalizations. The finite radiative correction coming from  $\mathcal{H}^T$  gives the following effects to the penguin-type on-shell quark amplitude [15,17,18]:

$$\sum_{i=3}^6 \langle c_i(\mu) O_i \rangle = \sum_{i=3}^6 c_i^{\text{eff}} \langle O_i \rangle^{\text{tree}}, \quad (13)$$

with

$$c_3^{\text{eff}} = c_3(\mu) - \frac{1}{3}P_s(k^2), \quad c_4^{\text{eff}} = c_4(\mu) + P_s(k^2), \quad c_5^{\text{eff}} = c_5(\mu) - \frac{1}{3}P_s(k^2), \quad c_6^{\text{eff}} = c_6(\mu) + P_s(k^2),$$

where  $P_s$  is given by:

$$P_s(k^2) = \frac{\alpha_s}{8\pi}c_2 \left[ \frac{10}{9} + 4 \int_0^1 dx x(1-x) \ln \frac{m_c^2 - x(1-x)k^2}{\mu^2} \right], \quad (14)$$

with  $m_c$  and  $k^2$  being charm quark mass and the gluon momentum, respectively. We neglect any finite radiative corrections coming from penguin Hamiltonian, as well as finite corrections to the tree amplitude, since they are suppressed by  $\alpha_s/4\pi$ . The choice of  $k^2$  is important for evaluating the strong phase at the quark level. In this work, we use  $k^2/m_b^2 = 0.5$  and  $k^2/m_b^2 = 0.3$ .

We neglect the effects of the electroweak penguin operators in this paper, since they are smaller than the uncertainties of the hadronic matrix estimation.

We start from the  $B^- \rightarrow \rho^0 \rho^-$  decay. Within the factorization approximation of the hadronic matrix elements, we obtain:

$$\begin{aligned} \langle \rho^0 \rho^- | \sum_{i=1}^2 c_i O_i | B^- \rangle &= (c_1 + c_2/N_c) \langle \rho^0 | \bar{u}_L \gamma^\mu u_L | 0 \rangle \langle \rho^- | \bar{d}_L \gamma_\mu b_L | B^- \rangle \\ &\quad + (c_1/N_c + c_2) \langle \rho^- | \bar{d}_L \gamma^\mu u_L | 0 \rangle \langle \rho^0 | \bar{u}_L \gamma_\mu b_L | B^- \rangle, \\ \langle \omega \rho^- | \sum_{i=1}^2 c_i O_i | B^- \rangle &= (c_1 + c_2/N_c) \langle \omega | \bar{u}_L \gamma^\mu u_L | 0 \rangle \langle \rho^- | \bar{d}_L \gamma_\mu b_L | B^- \rangle \\ &\quad + (c_1/N_c + c_2) \langle \rho^- | \bar{d}_L \gamma^\mu u_L | 0 \rangle \langle \omega | \bar{u}_L \gamma_\mu b_L | B^- \rangle, \end{aligned}$$

where we have neglected the annihilation diagram. Since the factorization approximation is not theoretically justified, we leave the color suppression factor ( $1/N_c$ ) as a free parameter. Actually, measurements of the branching fractions of  $B \rightarrow D$  decays indicate  $(c_1 + c_2/N_c)/(c_2 + c_1/N_c) \simeq 0.15$ , which implies  $N_c \simeq 2$  in the factorization assumption [19]. In this work, we use  $N_c = 2$  and  $N_c = \infty$ .

It is convenient to define

$$A(\epsilon_c, q_c, \epsilon_n, q_n) \equiv \langle \rho^0 | \bar{u}_L \gamma^\mu u_L | 0 \rangle \langle \rho^- | \bar{d}_L \gamma_\mu b_L | B^- \rangle,$$

where  $\epsilon_c$  and  $\epsilon_n$  are the polarization vector of  $\rho^-$  and  $\rho^0$ , respectively, and  $q_c$  and  $q_n$  are the four momentum of the  $\rho^-$  and  $\rho^0$ , respectively. By using the Lorentz structure of the

$\rho$ -meson form factor [20]  $\langle \rho^- | \bar{d}_L \gamma_\mu b_L | B^- \rangle$ , we can show  $A(\epsilon_c, q_c, \epsilon_n, q_n) \equiv A(\epsilon_n, q_n, \epsilon_c, q_c)$ .

The isospin  $U(2)$  symmetry thus leads to

$$\begin{aligned} \langle \rho^0 \rho^- | \sum_{i=1}^2 c_i O_i | B^- \rangle &= (1 + 1/N_c)(c_1 + c_2)A(\epsilon_c, q_c, \epsilon_n, q_n), \\ \langle \omega \rho^- | \sum_{i=1}^2 c_i O_i | B^- \rangle &= (1 + 1/N_c)(c_1 + c_2)A(\epsilon_c, q_c, \epsilon_n, q_n). \end{aligned}$$

The contributions from the penguin Hamiltonian can be evaluated in a similar manner:

$$\langle \rho^0 \rho^- | \sum_{i=3}^6 c_i O_i | B^- \rangle = 0 \quad (15)$$

$$\langle \omega \rho^- | \sum_{i=3}^6 c_i O_i | B^- \rangle = 2((1 + 1/N_c)c_3 + (1 + 1/N_c)c_4 + c_5 + c_6/N_c)A(\epsilon_c, q_c, \epsilon_n, q_n). \quad (16)$$

We thus obtain

$$\alpha e^{i\delta_\alpha} = 1, \quad \beta e^{i\delta_\beta} = 0, \quad r' e^{i\delta_q} = 2 \frac{(1 + 1/N_c)c_3 + (1 + 1/N_c)c_4 + c_5 + c_6/N_c}{(1 + 1/N_c)(c_1 + c_2)} \left| \frac{V_{tb}V_{td}^*}{V_{ub}V_{ud}^*} \right|. \quad (17)$$

We note that the  $\rho$ -meson polarization dependences on the hadronic parameters, e.g.,  $\alpha$ ,  $\beta$ , disappear in this  $U(2)$  symmetry approximation. The  $CP$ -odd angular coefficients [18] do not appear within this assumption.

In a similar manner, we evaluate the parameters of the  $B^- \rightarrow \rho^0 K^{*-}$  decay:

$$\begin{aligned} \alpha e^{i\delta_\alpha} &= 1, \quad \beta e^{i\delta_\beta} = \frac{c_3/N_c + c_4}{(2 + 1/N_c)c_3 + (1 + 2/N_c)c_4 + 2c_5 + 2c_6/N_c}, \\ r' e^{i\delta_q} &= \frac{(2 + 1/N_c)c_3 + (1 + 2/N_c)c_4 + 2c_5 + 2c_6/N_c}{(1 + 1/N_c)(c_1 + c_2)} \left| \frac{V_{tb}V_{ts}^*}{V_{ub}V_{us}^*} \right|, \end{aligned} \quad (18)$$

where we have neglected the  $U(3)$  breaking effects in the form factors.

For the  $B^- \rightarrow \rho^0 \pi^-$  and  $B^- \rightarrow \rho^0 K^-$  decays, we evaluate the matrix elements by using the form factors calculated in Ref. [20].

The numerical results are summarized in Tables I, II, III, and IV for  $N_c = 2, \infty$  and  $k^2/m_b^2 = 0.5, 0.3$ . We used  $m_u = 5\text{MeV}$ ,  $m_d = 8\text{MeV}$ ,  $m_s = 150\text{MeV}$ ,  $m_c = 1.35\text{GeV}$  and  $m_b = 5\text{GeV}$  in this calculation.

We next discuss how we can extract the weak phase from the observed  $CP$  asymmetries. The existence of the short distance absorptive part triggers a  $CP$  asymmetry in  $\Gamma(B^\pm \rightarrow \rho^0)$  and  $\Gamma(B^\pm \rightarrow \omega)$ : [18]

$$\frac{\Gamma(B^- \rightarrow \rho^0) - \Gamma(B^+ \rightarrow \rho^0)}{\Gamma(B^- \rightarrow \rho^0) + \Gamma(B^+ \rightarrow \rho^0)} = \frac{\beta r' (\cos(\delta_q + \delta_\beta + \phi) - \cos(\delta_q + \delta_\beta - \phi))}{1 + \beta^2 r'^2 + \beta r' (\cos(\delta_q + \delta_\beta + \phi) - \cos(\delta_q + \delta_\beta - \phi))}, \quad (19)$$

$$\frac{\Gamma(B^- \rightarrow \omega) - \Gamma(B^+ \rightarrow \omega)}{\Gamma(B^- \rightarrow \omega) + \Gamma(B^+ \rightarrow \omega)} = \frac{\alpha^{-1} r' (\cos(\delta_q - \delta_\alpha + \phi) + \cos(\delta_q - \delta_\alpha - \phi))}{1 + \alpha^{-2} r'^2 + \alpha^{-1} r' (\cos(\delta_q - \delta_\alpha + \phi) + \cos(\delta_q - \delta_\alpha - \phi))}. \quad (20)$$

We also obtain the ratio of partial decay width:

$$\frac{\Gamma(B^- \rightarrow \omega) + \Gamma(B^+ \rightarrow \omega)}{\Gamma(B^- \rightarrow \rho^0) + \Gamma(B^+ \rightarrow \rho^0)} = \frac{\alpha^2 + r'^2 + \alpha r' (\cos(\delta_q - \delta_\alpha + \phi) + \cos(\delta_q - \delta_\alpha - \phi))}{1 + \beta^2 r'^2 + \beta r' (\cos(\delta_q + \delta_\beta + \phi) + \cos(\delta_q + \delta_\beta - \phi))}. \quad (21)$$

Since the quark loop absorptive parts of the tree amplitudes are negligibly small, we can assume that  $\delta_\alpha = 0$ . We therefore have six unknown parameters  $(\alpha, \beta, \delta_\beta, \delta_q, r', \phi_i)$ . On the other hand, in addition to the above-mentioned observables, Eqs.(19)–(21), we can measure two  $M(\pi^+\pi^-)$  spectra ( for  $B^-$  and  $B^+$  ) around  $M(\omega) \pm \Gamma(\omega)$  due to  $\rho - \omega$  interference; each provides two types of information, i.e., the pole position and magnitude. We can, therefore, derive the weak phase  $\phi_i$  ( $i = 2, 3$ ) from these measurements without assuming any theoretical models of the hadron matrix elements. We also note that the existence of the electroweak penguin operators does not affect this determination. For most of decay modes we can also assume  $\alpha = 1$ , which improves the accuracy of the  $\phi_i$  determination.

We demonstrate the asymmetry patterns ( $\pi^+\pi^-$  invariant mass spectra) in Figures 2 (a1)-(d3), where (a), (b), (c), and (d) denote  $B^- \rightarrow \rho^0 \rho^+$ ,  $\rho^0 K^{*-}$ ,  $\rho^0 K^-$ , and  $B^0 \rightarrow \rho^0 \bar{K}^0$  decay modes, respectively. The results using the numerical values of Table I are given in Figures 2 (a1), (b1), (c1), and (d1) and those of Table III are shown in Figures 2 (a3), (b3), (c3), and (d3). In Figures 2 (a2), (b2), (c2), and (d2), we used “zero hadronic phases” (i.e.,  $\delta_\beta, \delta_q = 0$  or  $\pm\pi$ ) with  $\alpha, \beta$ , and  $r'$  from Table I. The solid lines are for  $B^+$  or  $B$  and the dashed ones are for  $B^-$  or  $\bar{B}$ . Here, we have assumed the KM matrix of Wolfenstein parametrization,  $\lambda = 0.221$ ,  $\rho = -0.12$ ,  $\eta = 0.34$  and  $A = 0.84$ , which corresponds to  $(\phi_1, \phi_2, \phi_3) = (15, 55, 110)$  degrees. The branching ratios in these parameters are given in Table V. The vertical scales are normalized to give the number of entries at  $10^8 B\bar{B}$  events with an 100-% acceptance. Drastic asymmetries appear around the  $\omega$  mass region.

We list the asymmetries obtained for the various decay modes in Table V. The hadronic parameters in Tables I – IV are assumed.  $A(\rho^0)$  and  $A(\omega)$  are the asymmetries of the  $\rho^0 h$  and



$\omega h$  modes.  $A(\rho\omega)$  is the mean asymmetry of the  $M(\pi^+\pi^-)$  invariant mass spectra around  $M(\omega) \pm \Gamma(\omega)$ , and  $A^{max}(\rho\omega)$  is the maximum asymmetry in this region.  $A^0(\rho\omega)$  is obtained by assuming the “zero hadronic phase”. The branching ratios are also estimated using this formalism. The  $CP$  asymmetries via  $\rho$ - $\omega$  interference are large ( $> 10\%$ ) in most of cases.

In order to check the feasibility for detecting this  $CP$  asymmetry, we performed a simulation assuming the BELLE detector of the KEK B-factory [3], an asymmetric  $e^+e^-$  collider ( $8 \times 3.5\text{GeV}$ ). The invariant mass resolution of  $\pi^+\pi^-$  around  $\omega$  mass is expected to be 3.2 MeV for the  $B \rightarrow \omega h$ ,  $\omega \rightarrow \pi^+\pi^-$  decay; this is enough to resolve the interference pattern. Here, the momentum resolution is derived from  $(dP_T/P_T)^2 = (0.001P_T/1\text{GeV})^2 + 0.002^2$ . In the case of a symmetric collider, the mass resolution will be better. In case of hadron machine, the average  $B$  mesons’  $P_T$  would be several GeV or more. Although the mass resolution slightly deteriorates, the statistics are sufficient in hadron machines.

In order to suppress the large background from continuum events under  $\Upsilon(4S)$ , we used two cuts in analysing the  $\rho^0 h^{\pm,0}$  decay [21]: one was that the absolute value of the cosine of the angle between the thrust axes of  $B$  decay products and the other particles at center-of-mass-system of  $\Upsilon(4S)$  be less than 0.6; the other was that the energy of the  $B$  candidate be between 5.25 and 5.325 GeV. The combined efficiency of these two cuts was 60%. The beam-energy constraint mass spectra were used. The acceptances of  $\rho^0\pi^\pm$  and  $\rho^0K^\pm$  were found to be  $\sim 35\%$ . The efficiency of charged track is typically 80% and that of  $\pi^0 \sim 33\%$ . The backgrounds from  $\Upsilon(4S)$  decay, i.e.,  $B\bar{B}$  events, are mostly  $h^-\bar{D}(\bar{D} \rightarrow K^-\pi^+, K^-\rho^+, \dots)$ . We can, therefore, reject combinations if there are possible combination including  $K^-$ , which have masses consistent with  $D$  or  $D^*$ . This cut does not deteriorate the acceptances.

The results of a simulation for  $B^\pm \rightarrow \rho^0 h^\pm$  ( $h^\pm = \pi^\pm, \rho^\pm, K^\pm, K^{*\pm}$ ) decay modes are summarized in  $N(B\bar{B})$  of Table V, the necessary number of  $B\bar{B}$  events for detecting the  $3\sigma$   $CP$  asymmetry at the  $\rho$ - $\omega$  interference region. The branching ratios quoted in Table V are assumed. In some of these decay modes,  $3\sigma$ -CP violations are detectable with  $10^9$   $B\bar{B}$  events by  $\rho - \omega$  interference modes. A luminosity of  $10^{35} \text{cm}^{-2} \text{s}^{-1}$  is necessary. It may be possible if the experimental setup (including accelerator’s setup) is optimized for the

detection of direct  $CP$  violations. Also, in these decay modes, direct  $CP$  violations via  $B \rightarrow \omega h, \omega \rightarrow \pi^+\pi^-\pi^0$  can be detected with the same luminosity if their asymmetries are on the order of 10% or larger. This is because both the  $\rho$ - $\omega$  interference and the  $\omega$ -peak are narrow, which reduces the background. If a good method can be found to suppress the background from the continuum, the necessary luminosity can be significantly reduced. This is due to large  $CP$  asymmetries via  $\rho - \omega$  interference, which is less sensitive to theoretical assumptions. If these things are realized, we can determine  $\phi_i$  ( $i = 2, 3$ ), as we previously discussed.

The advantage of this method are as follows:

- The behavior of the final state interaction can be controlled by using the  $\omega$  meson pole. This method is insensitive to the ambiguity of other hadronic phases, which can be calculated from experimental data.
- $\phi_2$  and  $\phi_3$  can be measured by the Cabibbo-allowed and Cabibbo-suppressed channels, respectively. We also note that the direct  $CP$  asymmetry discussed in this paper is proportional to  $\sin \phi_i$ , which makes it possible to measure the weak phases for  $\phi_i \simeq \pi/2$ . In the case of indirect  $CP$  violation, asymmetry is proportional to  $\sin 2\phi_i$  [2].
- The typical experimental detector has some material in front of the central tracking device. This causes a systematic difference between the  $h^+$  and  $h^-$  yields. The present method looks only at the  $M(\pi^+\pi^-)$  shape, i.e., insensitive to these systematic effects. Only statistics and a high mass resolution are necessary.
- No tagging of the other B meson, nor the vertex chambers, to measure such a small decay length as  $\sim$ pico-second of B meson is essential.

We have studied the effect of  $\rho$ - $\omega$  interference in the decay modes  $B \rightarrow \rho^0(\omega)h, \rho^0(\omega) \rightarrow \pi^+\pi^-$ , where  $h$  is any hadronic final state, such as  $\pi, \rho$ , or  $K$ . Although the isospin-violating decay of  $\omega \rightarrow \pi^+\pi^-$  is a small effect with BR=2.2%, the interference at the kinematical region  $M(\pi^+\pi^-) \sim M(\omega) \pm \Gamma_\omega$  is enhanced by the  $\omega$  pole. We have shown the  $CP$  asymmetry to

be sufficiently large to be detected. The  $CP$  asymmetry appears in the deformation of the Breit-Wigner shape of the  $\rho^0 \rightarrow \pi^+\pi^-$  invariant mass spectrum. The prediction of the  $CP$  asymmetry is not very sensitive to the hadronic phase calculation, i.e., a “sure” prediction. Any B-factory, even if it is a symmetric  $e^+e^-$  collider or hadron machine, can carry out this measurement. We only need to accumulate enough statistics and to have a mass resolution  $[\Delta M(\pi^+\pi^-)]$  better than the width of the  $\omega$  meson (8.4MeV) at around the  $\omega$  mass region. An attempt to obtain more than  $10^9 B\bar{B}$  is important.

We thank Drs. M. Kobayashi, A. I. Sanda, M. Tanaka and I. Dunietz for useful discussions. We also thank Belle collaboration for providing detector simulation programs. M.T. is supported from Japanese Ministry of Education, Science and Culture for his stay at Fermilab. He thanks Fermilab Theoretical Physics Group for hospitality.

## REFERENCES

- [1] M. Kobayashi and T. Maskawa, Prog. Theor. Phys. **49** (1973) 652.
- [2] A. B. Carter and A. I. Sanda, Phys. Rev. Lett. **45** (1980) 952; Phys. Rev. **D23** (1981) 1567; I. I. Bigi and A. I. Sanda, Nucl. Phys. **B193** (1981) 85.
- [3] Belle collaboration, “A study of  $CP$  violation in B meson decays; the technical design report”, KEK report 95-1.
- [4] BABAR collaboration, “BABAR technical design report”, SLAC-R-95-457.
- [5] T. Lohse et al., “HERA B: An experiment to study  $CP$  violation in the B system using an internal target at the HERA proton ring: Proposal”, DESY PRC-94-02.
- [6] D. Atwood and A. Soni, Z. Phys. **C 64** (1994) 241.
- [7] D. Atwood and A. Soni, Phys. Rev. Lett. **74** (1995) 220.
- [8] G. Eilam, M. Gronau, and R. R. Mendel, Phys. Rev. Lett. **74** (1995) 4984.
- [9] H.J. Lipkin, hep-ph/9310318, WIS-93-107-PH.
- [10] Y. Nambu and J. J. Sakurai, Phys. Rev. Lett. **8** (1962) 79; For a recent review, see H.B. O’Connell, hep-ph/9604375.
- [11] A. Deandrea, N. Di Bartolomeo and R. Gatto, Phys. Lett. **B318** (1993) 549; A. Deandrea et al., Phys. Lett. **B320** (1994) 170.
- [12] N. G. Deshpande and J. Trampetic, Phys. Rev. **D41** (1990) 895.
- [13] M. Bander, D. Silverman and A. Soni, Phys. Rev. Lett. **43** (1979) 242.
- [14] J. Gasser and H. Leutwyler, Phys. Rep. **87** (1982) 77.
- [15] N.G. Deshpande and X-G. He, Phys. Rev. Lett. **74** (1995) 26.
- [16] A. Buras, M. Jamin, M. Lautenbacher and P. Weisz, Nucl. Phys. **B400** (1993) 37; A.

- Buras, M.Jamin and M. Lautenbacher, Nucl. Phys. **B400** (1993) 75.
- [17] R. Fleischer, Z.Phys. **C58** (1993) 483; Z.Phys. **C62** (1994) 81.
- [18] G. Kramer, W.F. Palmer and H. Simma, Nucl. Phys. **B428** (1994) 77; Z. Phys. **C66** 429.
- [19] J.L. Rodriguez, hep-ex/9604011.
- [20] M. Bauer, B. Stech and M. Wirbel, Z. Phys. **C34** (1987) 103; M. Wirbel, B. Stech and M. Bauer, Z. Phys. **C29** (1985) 637.
- [21] D. M. Asner et al., Phys. Rev. **D53** (1996) 1039.

TABLES

	$\alpha$	$\beta$	$\delta_\beta$	$r'$	$\delta_q$
$B^- \rightarrow \rho^0 \rho^-$	1.	0.	—	$9.6 \times 10^{-2}  (V_{tb} V_{td}^*) / (V_{ub} V_{ud}^*) $	-2.807
$B^- \rightarrow \rho^0 K^{*-}$	1.	0.524	0.020	$6.3 \times 10^{-2}  (V_{tb} V_{ts}^*) / (V_{ub} V_{us}^*) $	-2.814
$B^- \rightarrow \rho^0 \pi^-$	1.	0.423	3.103	$1.0 \times 10^{-1}  (V_{tb} V_{td}^*) / (V_{ub} V_{ud}^*) $	-2.796
$B^- \rightarrow \rho^0 K^-$	1.	0.117	0.343	$4.8 \times 10^{-2}  (V_{tb} V_{ts}^*) / (V_{ub} V_{us}^*) $	-2.792
$\bar{B}^0 \rightarrow \rho^0 \pi^0$	0.262	2.035	3.138	$9.5 \times 10^{-2}  (V_{tb} V_{td}^*) / (V_{ub} V_{ud}^*) $	-2.805
$\bar{B}^0 \rightarrow \rho^0 \bar{K}^0$	1.	0.126	-2.830	$1.63 \times 10^{-1}  (V_{tb} V_{ts}^*) / (V_{ub} V_{us}^*) $	-2.793

TABLE I.  $N_c = 2$ ,  $k^2 = 0.5m_b^2$

	$\alpha$	$\beta$	$\delta_\beta$	$r'$	$\delta_q$
$B^- \rightarrow \rho^0 \rho^-$	1.	0.	—	$3.5 \times 10^{-2}  (V_{tb} V_{td}^*) / (V_{ub} V_{ud}^*) $	-2.749
$B^- \rightarrow \rho^0 K^{*-}$	1.	2.270	-3.060	$2.8 \times 10^{-2}  (V_{tb} V_{ts}^*) / (V_{ub} V_{us}^*) $	0.247
$B^- \rightarrow \rho^0 \pi^-$	1.	3.082	0.183	$3.9 \times 10^{-1}  (V_{tb} V_{td}^*) / (V_{ub} V_{ud}^*) $	0.122
$B^- \rightarrow \rho^0 K^-$	1.	0.126	-2.964	$1.64 \times 10^{-1}  (V_{tb} V_{ts}^*) / (V_{ub} V_{us}^*) $	0.284
$\bar{B}^0 \rightarrow \rho^0 \pi^0$	0.262	1.413	0.030	$1.44 \times 10^{-1}  (V_{tb} V_{td}^*) / (V_{ub} V_{ud}^*) $	-2.851
$\bar{B}^0 \rightarrow \rho^0 \bar{K}^0$	1.	0.136	0.168	$2.13 \times 10^{-1}  (V_{tb} V_{ts}^*) / (V_{ub} V_{us}^*) $	-2.858

TABLE II.  $N_c = \infty$ ,  $k^2 = 0.5m_b^2$

	$\alpha$	$\beta$	$\delta_\beta$	$r'$	$\delta_q$
$B^- \rightarrow \rho^0 \rho^-$	1.	0.	—	$1.1 \times 10^{-1}  (V_{tb}V_{td}^*)/(V_{ub}V_{ud}^*) $	-3.056
$B^- \rightarrow \rho^0 K^{*-}$	1.	0.527	0.005	$7.2 \times 10^{-2}  (V_{tb}V_{ts}^*)/(V_{ub}V_{us}^*) $	-3.058
$B^- \rightarrow \rho^0 \pi^-$	1.	0.420	3.133	$1.15 \times 10^{-1}  (V_{tb}V_{td}^*)/(V_{ub}V_{ud}^*) $	-3.054
$B^- \rightarrow \rho^0 K^-$	1.	0.119	0.075	$5.5 \times 10^{-2}  (V_{tb}V_{ts}^*)/(V_{ub}V_{us}^*) $	-3.053
$\bar{B}^0 \rightarrow \rho^0 \pi^0$	0.262	2.033	3.141	$1.1 \times 10^{-1}  (V_{tb}V_{td}^*)/(V_{ub}V_{ud}^*) $	-3.056
$\bar{B}^0 \rightarrow \rho^0 \bar{K}^0$	1.	0.128	-3.074	$1.87 \times 10^{-1}  (V_{tb}V_{ts}^*)/(V_{ub}V_{us}^*) $	-3.053

TABLE III.  $N_c = 2$ ,  $k^2 = 0.3m_b^2$

	$\alpha$	$\beta$	$\delta_\beta$	$r'$	$\delta_q$
$B^- \rightarrow \rho^0 \rho^-$	1.	0.	—	$4.1 \times 10^{-2}  (V_{tb}V_{td}^*)/(V_{ub}V_{ud}^*) $	-3.043
$B^- \rightarrow \rho^0 K^{*-}$	1.	2.323	-3.123	$3.1 \times 10^{-2}  (V_{tb}V_{ts}^*)/(V_{ub}V_{us}^*) $	0.065
$B^- \rightarrow \rho^0 \pi^-$	1.	3.291	0.045	$4.2 \times 10^{-2}  (V_{tb}V_{td}^*)/(V_{ub}V_{ud}^*) $	0.034
$B^- \rightarrow \rho^0 K^-$	1.	0.131	-3.102	$1.86 \times 10^{-1}  (V_{tb}V_{ts}^*)/(V_{ub}V_{us}^*) $	0.074
$\bar{B}^0 \rightarrow \rho^0 \pi^0$	0.262	1.424	0.007	$1.63 \times 10^{-1}  (V_{tb}V_{td}^*)/(V_{ub}V_{ud}^*) $	-3.066
$\bar{B}^0 \rightarrow \rho^0 \bar{K}^0$	1.	0.140	0.038	$2.43 \times 10^{-1}  (V_{tb}V_{ts}^*)/(V_{ub}V_{us}^*) $	-3.068

TABLE IV.  $N_c = \infty$ ,  $k^2 = 0.3m_b^2$

Mode	Table	BR	$A(\rho^0)$	$A(\omega)$	$A(\rho\omega)$	$A^{max}(\rho\omega)$	$A^0(\rho\omega)$	$N(B\bar{B})$
		$\times 10^{-8}$	%	%	%	%	%	$\times 10^8$
$B^- \rightarrow \rho^0 \rho^-$	I	2100	0	10	13	26	11	70
$B^- \rightarrow \rho^0 K^{*-}$	I	720	-36	-19	-45	-79	-19	12
$B^- \rightarrow \rho^0 \pi^-$	I	660	-6	11	16	37	18	29
$B^- \rightarrow \rho^0 K^-$	I	62	-41	-26	-82	-91	-67	7.6
$B^- \rightarrow \rho^0 \rho^-$	II	910	0	5	5	9	4	1900
$B^- \rightarrow \rho^0 K^{*-}$	II	840	-19	16	10	32	28	490
$B^- \rightarrow \rho^0 \pi^-$	II	170	-21	-2	-5	-17	13	2600
$B^- \rightarrow \rho^0 K^-$	II	33	-59	5	33	58	31	15
$B^- \rightarrow \rho^0 \rho^-$	III	2100	0	3	14	30	13	61
$B^- \rightarrow \rho^0 K^{*-}$	III	780	-9	-4	-23	-57	-17	42
$B^- \rightarrow \rho^0 \pi^-$	III	660	-2	3	20	48	21	16
$B^- \rightarrow \rho^0 K^-$	III	56	-13	-6	-70	-82	-65	11
$B^- \rightarrow \rho^0 \rho^-$	IV	910	0	2	5	11	5	1900
$B^- \rightarrow \rho^0 K^{*-}$	IV	970	-4	4	20	40	24	98
$B^- \rightarrow \rho^0 \pi^-$	IV	170	-31	-7	-12	-27	16	440
$B^- \rightarrow \rho^0 K^-$	IV	33	-15	1	28	48	28	17

TABLE V. Asymmetries for the various decay modes; Table denotes the Table number for hadronic parameters, and BR is branching ratios in unit of  $10^{-8}$ .  $A(\rho^0)$  and  $A(\omega)$  are asymmetries for  $B^- \rightarrow \rho^0 h$  and  $\omega h$  modes, respectively.  $A(\rho\omega)$  is that in the region of  $M(\omega) \pm \Gamma(\omega)$ .  $A^{max}(\rho\omega)$  is the maximum asymmetry in this region.  $A^0(\rho\omega)$  is that under assumption of “zero hadronic phase”.  $N(B\bar{B})$  is a necessary number of  $B\bar{B}$  events in order to obtain a  $3\sigma$  asymmetry in  $\rho - \omega$  interference region.



FIGURES

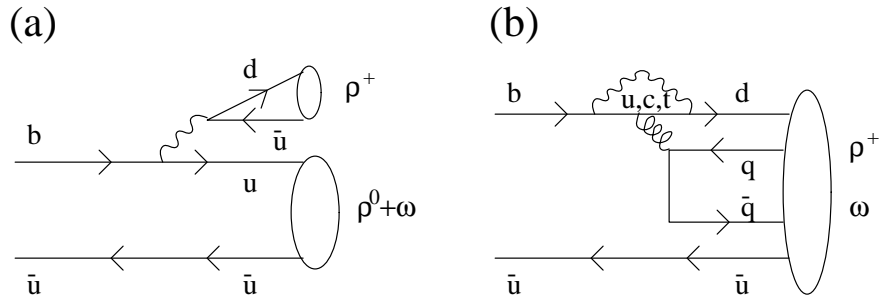


FIG. 1. Examples of the Feynman diagrams of the decay  $B^- \rightarrow \rho^0(\omega)\rho^-$ ; (a) tree and (b) penguin diagram.

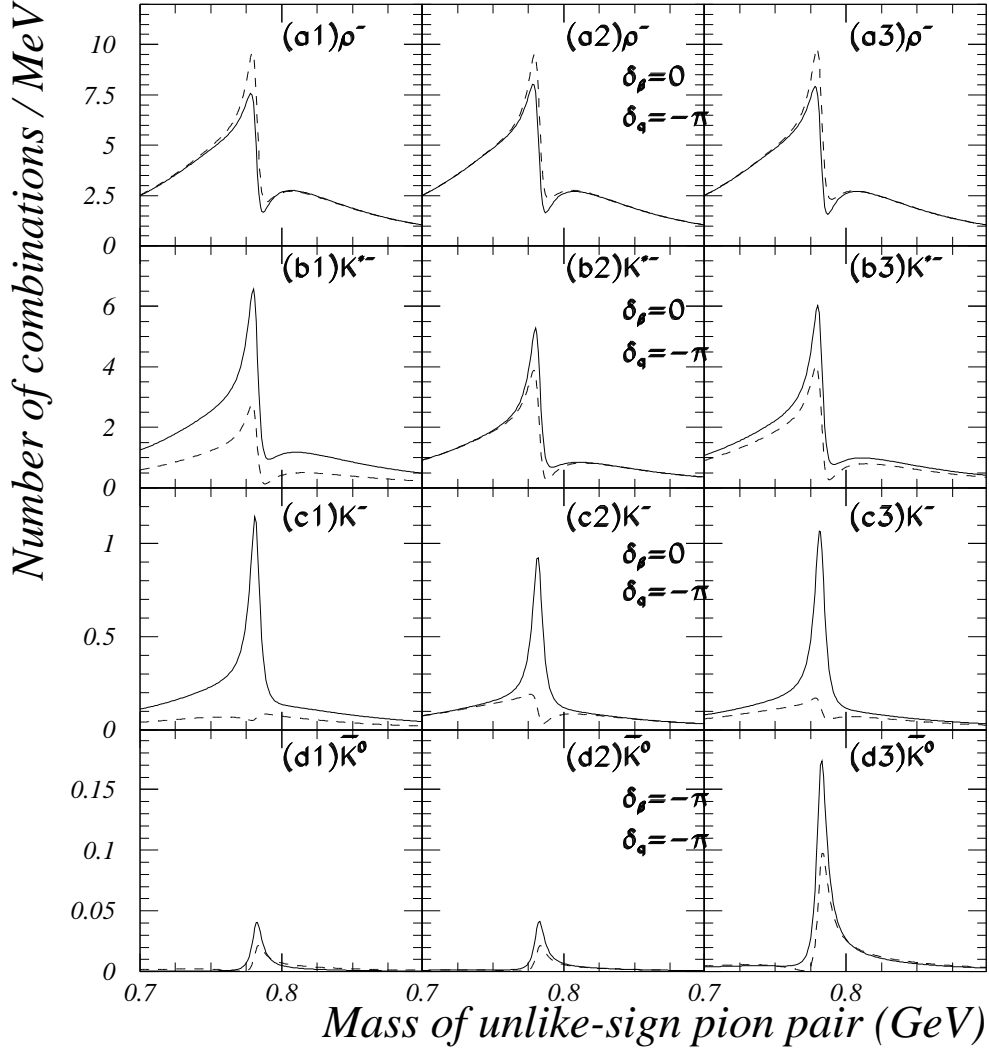


FIG. 2. Expected invariant mass spectra of unlike-sign pion pairs. The solid lines are for  $B^+$  or  $B^0$  decays, and the dashed ones are for  $B^-$  or  $\bar{B}^0$  decays. The vertical scale is the differential yield for  $(\pi^+\pi^-)h^{\pm,0}$  combinations, and is normalized to give the number of entries at  $10^8 B\bar{B}$  events, assuming an 100-% acceptance. The details concerning the notations (a1)-(d3) are described in the text.